



Pathogenesis of holoprosencephaly

Xin Geng and Guillermo Oliver

Department of Genetics and Tumor Cell Biology, St. Jude Children's Research Hospital, Memphis, Tennessee, USA.



Holoprosencephaly (HPE), the most common human forebrain malformation, occurs in 1 in 250 fetuses and 1 in 16,000 live births. HPE is etiologically heterogeneous, and its pathology is variable. Several mouse models of HPE have been generated, and some of the molecular causes of different forms of HPE and the mechanisms underlying its variable pathology have been revealed by these models. Herein, we summarize the current knowledge on the genetic alterations that cause HPE and discuss some important questions about this disease that remain to be answered.

Development of the forebrain

Holoprosencephaly (HPE) is a developmental disorder, and interpretation of its pathogenesis requires a clear understanding of normal forebrain development (Figure 1). During early embryogenesis, the mouse blastocyst develops into a bilayered conical structure, with the epiblast inside and the visceral endoderm outside (Figure 1A). As development progresses, a group of visceral endodermal cells located at the distal tip of the egg cylinder moves anteriorly to form the anterior visceral endoderm, while the primitive streak forms at the posterior epiblast (Figure 1A). Subsequently, gastrulation occurs and epiblast cells ingress through the primitive streak (1, 2) (Figure 1A). As gastrulation progresses, neural specification results in the formation of the neural plate (3–5). The neural plate initially has an anterior identity (3–5), but signaling molecules from the posterior epiblast and lateral mesoderm subsequently induce posterior characteristics in this structure. Antagonists secreted mainly by the anterior visceral endoderm maintain and stabilize the fate of the anterior neuroectoderm (ANE), from which the forebrain arises (3, 4) (Figure 1, A and D).

Unlike the conical structure of the mouse blastocyst, that of the human blastocyst is a flat, bilayered disc (6) (Figure 1, B and C). Despite these differences in shape, the epiblast cells of both organisms undergo similar cell movements, and gastrulation initiates at the posterior end of both embryos (6) (Figure 1, B and C). The anterior hypoblast of the rabbit embryo, which is also a flat, disc-shaped structure, has head-inducing activity (7); thus, it is possible that the anterior hypoblast of human embryos is the functional equivalent of the mouse anterior visceral endoderm.

Toward the end of gastrulation, the embryo contains the three primary germ layers: the ectoderm, mesoderm, and endoderm. The axial mesoderm consists of the prechordal plate (PrCP) anteriorly and the notochord posteriorly (Figure 1D). The neural plate folds upon itself to form the neural tube, the anterior end of which subsequently expands and bifurcates to form the telencephalon (8, 9) (Figure 1, E and F). By the end of somatogenesis, the forebrain is

comprised by the telencephalon, diencephalon, and hypothalamus (3, 4, 10, 11) (Figure 1F). The dorsal telencephalon will develop into the cerebral cortex; the ventral telencephalon will develop into the basal ganglia; and the olfactory bulbs will form the most anterior portion of the cerebrum in mouse and in human it lies underneath the frontal lobe (Figure 1, G–J).

Overview of HPE

HPE is defined as the incomplete separation of the two cerebral hemispheres. Based on the severity of the defect, HPE is subgrouped into three forms (12–16): alobar, semilobar, and lobar HPE. Alobar HPE, the most severe form, is characterized by the presence of a small single cerebral ventricle that lacks interhemispheric division, corpus callosum, and olfactory bulbs (17, 18) (Figure 2, compare A–C and D–F). In semilobar HPE, the moderate form, the frontoparietal lobes fail to separate; however, the interhemispheric fissure is present posteriorly, and the olfactory bulbs and corpus callosum are either absent or hypoplastic (underdeveloped) (17) (Figure 2, G–I). In lobar HPE, the mild form, a distinct interhemispheric fissure is present; however, some midline continuity of the cingulate gyrus persists (Figure 2, J and K).

Eighty percent of HPE cases are associated with facial abnormalities. Cyclopia, proboscis (a tubular appendage located above the eye), and cleft lip/palate are associated with severe forms of HPE (19, 20) (Figure 2, M and N). Ocular hypotelorism (an abnormal decrease in the distance between both eyes), nasal abnormalities, and a single central maxillary incisor are associated with minor forms of HPE (19–21) (Figure 2, O–Q). Milder craniofacial features that occur in the absence of forebrain defects are called microforms (12–16, 19, 20) (Figure 2, P and Q). A middle interhemispheric variant of HPE (MIH), also known as syntelencephaly, is also observed in humans. In MIH, the defects in cerebral hemisphere separation occur only at the posterior frontal and parietal regions; the anterior frontal and occipital lobes separate normally (22–24) (Figure 2, L and R).

Etiology of HPE. The etiology of HPE includes genetic and environmental causes. The environmental risk factors include maternal diabetes, maternal alcoholism, and prenatal exposure to drugs (e.g., retinoic acid, cholesterol biosynthesis inhibitors) (25). HPE is inherited as an autosomal-dominant disease. Mutations in the following nine genes have been identified in patients with HPE: sonic hedgehog (*SHH*), patched homolog 1 (*PTCH1*), glioma-associated oncogene family zinc finger 2 (*GLI2*), teratocarcinoma-derived growth factor 1 (*TDGF1*, also known as *CRIPTO*), TGF- β -induced factor homeobox 3 (*TGIF*), forkhead box H1 (*FOXH1*), zinc finger protein of the cerebellum 2 (*ZIC2*), SIX homeobox 3 (*SIX3*), and

Conflict of interest: The authors have declared that no conflict of interest exists.

Nonstandard abbreviations used: ANE, anterior neuroectoderm; Bmp, bone morphogenetic protein; Cdo, cell adhesion molecule-related/downregulated by oncogenes; Chd, chordin; FOXH1, forkhead box H1; Gas1, growth arrest-specific 1; Gdf1, growth differentiation factor 1; GLI2, glioma-associated oncogene family zinc finger 2; HPE, holoprosencephaly; LGE, lateral ganglionic eminence; MGE, median ganglionic eminence; MIH, middle interhemispheric variant of HPE; Nkx2.1, NK2 homeobox 1; Nog, noggin; PrCP, prechordal plate; SHH, sonic hedgehog; SIX3, SIX homeobox 3; TDGF1, teratocarcinoma-derived growth factor 1; TGIF, TGF- β -induced factor homeobox 3; Tsg, twisted gastrulation; ZIC2, zinc finger protein of the cerebellum 2.

Citation for this article: *J. Clin. Invest.* 119:1403–1413 (2009). doi:10.1172/JCI38973.

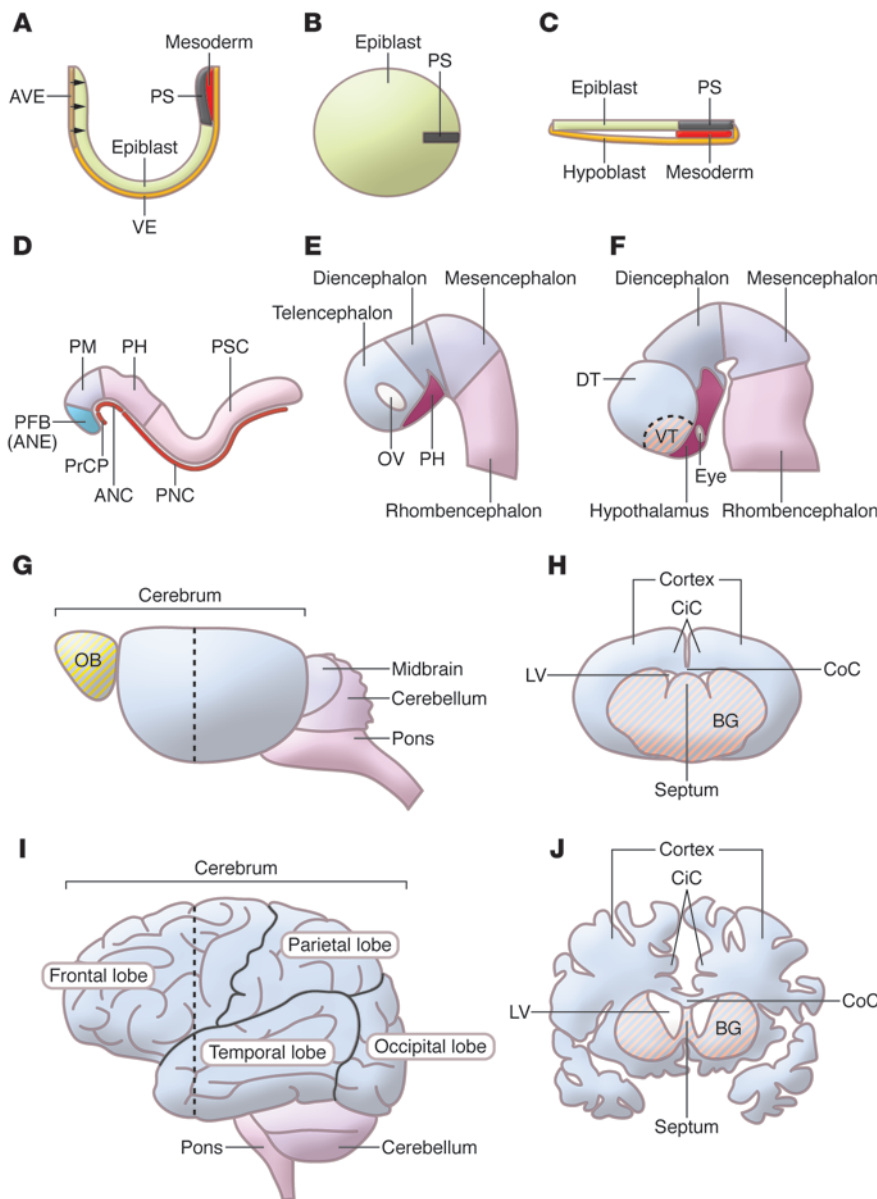


Figure 1

Development of the mammalian forebrain. (A–C) At early primitive-streak stage, epiblast cells ingress through the primitive streak (PS) to form the mesoderm. Medial sagittal section of E6.5 mouse (A) and Carnegie Stage 7 (CS7) human (B) embryos with anterior to the left. (C) Dorsal view of a CS7 human embryo. AVE, anterior visceral endoderm; VE, visceral endoderm. (D) At early somite stage (E8.5 for mouse; CS10 for human), the neural ectoderm has been specified into different regions along the anterior-posterior axis and the axial mesoderm is underlying the midline of the neural ectoderm. ANC, anterior notochord; PFB, prospective forebrain (or ANE); PH, prospective hindbrain; PM, prospective midbrain; PNC, posterior notochord; PSC, prospective spinal chord. (E) Neural tube closure occurs at around the 15-somite stage (E9.0 for mouse; CS11 for human). The forebrain gets further regionalized into telencephalon, diencephalon, and prospective hypothalamus (PH). OV, optic vesicle. (F) Approximately at E10.5 in the mouse or at CS14 in human embryos, the expanding telencephalon bifurcates dorsally to form the two hemispheres and gets patterned into dorsal telencephalon (DT) and ventral telencephalon (VT). (G and I) Lateral views of adult mouse (G) and human brain (I). OB, olfactory bulb. Black dashed lines in G and I indicate the location of coronal sections shown in H and J. (H and J) Coronal sections of adult mouse (H) and human brain (J). BG, basal ganglia; CiC, cingulate cortex; CoC, corpus callosum; LV, lateral ventricle.

dispatched homolog 1 (*DISP1*) (13–16, 26–28). Only about 28% of HPE cases are caused by mutations of these genes; thus, other genetic and/or environmental factors probably contribute to this malformation (15). Mild HPE is observed in a few (2%–4%) patients with Smith-Lemli-Opitz syndrome, which is caused by defects in the 7-dehydrocholesterol reductase (*DHCR7*) gene (14, 27).

Pathology of HPE. HPE phenotypes vary greatly, even across familial forms. Among consanguineous obligate mutation carriers, about 37% have HPE, 27% display microforms, and 36% have no clinical manifestation (16). The cause(s) of this variability remains unknown.

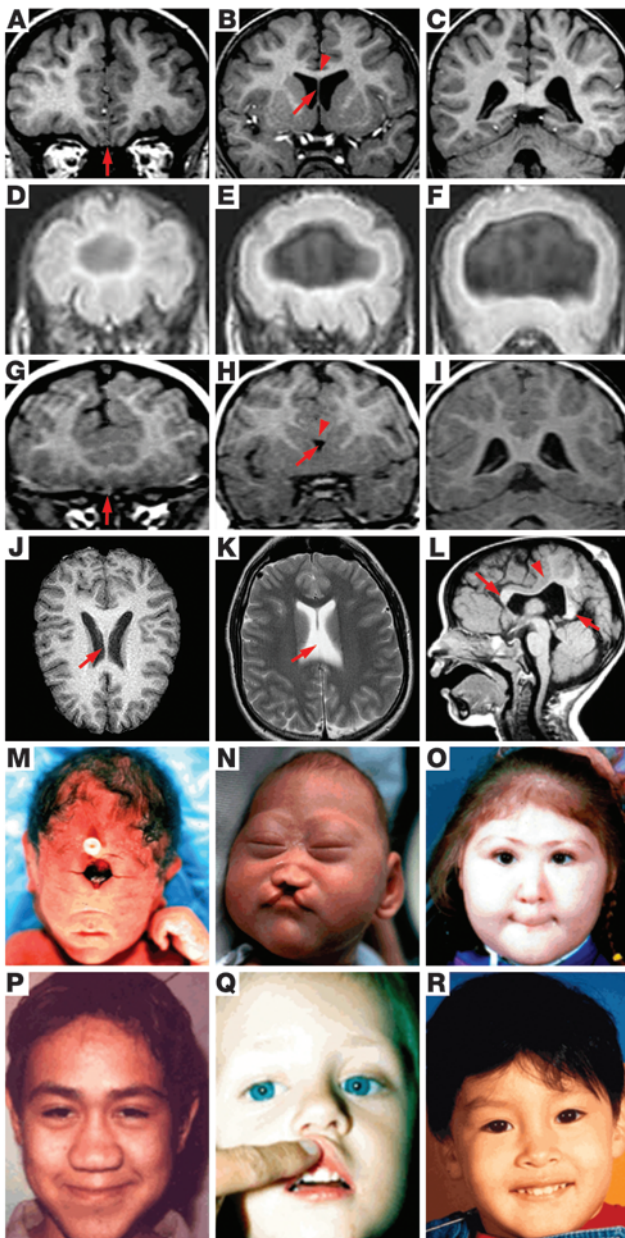
Diagnosis of HPE. Prenatal diagnosis of HPE is primarily based on ultrasound and MRI. Ultrasound can detect severe HPE as early as the first trimester but is less sensitive to milder forms of HPE. Fetal MRI better characterizes HPE malformations during the third trimester (15). Genetic diagnosis is currently not practical because of the etiologic heterogeneity and pathologic variability of HPE (15).

Current mouse models of HPE

Several mouse models of HPE have been generated during the last decade. Most were generated by genetic alterations, though some were obtained through the use of chemicals (29–33). In this Review, we will focus on only those mouse models generated using genetic approaches (Table 1 and Figure 3). Based on phenotypic criteria established in humans, the available mouse models can be separated into those that exhibit alobar HPE- or semilobar HPE-like phenotypes and those that exhibit microforms or MIH.

Mouse models exhibiting an alobar HPE-like phenotype

Nodal signaling pathway. Nodal is a member of the TGF- β superfamily. It signals through a heterodimer of type I serine-threonine kinase receptor, activin A receptor, type 1B (ActR1B) and type 2 receptors ActR2A or ActR2B in the presence of the coreceptor Cripto/Tdgf1 (Figure 4) (34). The binding of Nodal to the receptor complex leads to the phosphorylation of ActR1B by ActR2A/B. In

**Figure 2**

Clinical manifestations of HPE. (A–I) Coronal images of control and HPE brains from anterior (A, D, and G) to posterior (C, F, and I). (A–C) In the control brain, the two hemispheres are separated completely (arrow in A) and the septum (arrow in B) and the corpus callosum (arrowhead in B) are present. (D–F) In alobar HPE, a single cerebral ventricle is present and the interhemispheric fissure is completely absent. (G–I) In semilobar HPE, the two hemispheres are incompletely separated (arrow in G) and the septum and corpus callosum are absent (arrow and arrowhead in H, respectively). (J and K) Horizontal images of control (J) and lobar HPE (K). The septum is present in the control brain (arrow in J); however, it is partially absent in the lobar HPE brain (arrow in K). (L) Sagittal image of a MISH brain. The genu and splenium of the corpus callosum are present (arrows in L); however, the corpus callosum is absent at the region lacking the interhemispheric fissure (arrowhead in L). (M–O) Craniofacial defects associated with HPE. (M) Alobar HPE with cyclopia and proboscis. (N) Semilobar HPE with microcephaly and cleft lip and palate. (O) Semilobar HPE with ocular hypotelorism and midface hypoplasia. (P and Q) Microforms of HPE. (P) Absence of nasal bones and cartilage with a narrow nasal bridge. (Q) Single central maxillary incisor. (R) MISH patient with normal facial appearance. A–C and G–I are reprinted with permission from *Cerebral cortex* (17); D–F are reprinted with permission from *American Journal of Medical Genetics* (18); J is reprinted with permission from *Brain Maps* (111); K is reprinted with permission from *MedPix* (112); L is reprinted with permission from *American Journal of Neuroradiology* (23); M and O are reprinted with permission from *Human Molecular Genetics* (19); N and P are reprinted with permission from *Human Molecular Genetics* (20); Q is reprinted with permission from *Nature Genetics* (21); and R is reprinted with permission from *Human Molecular Genetics* (24).

turn, ActR1B phosphorylates Smad2 and Smad3, which then interact with Smad4 and activate downstream genes by recruiting transcriptional activators such as FoxH1 (Figure 4A) (34). Mutations in genes encoding key components of the Nodal signaling pathway, such as *Cripto/Tdgf1* and *FoxH1*, have been identified in patients with HPE (14–16, 26). Early work in zebrafish has revealed a connection between cyclopia and Nodal signaling (35–37). In mice, inactivation of the Nodal signaling pathway by genetic deletion of key components causes early embryonic lethality due to defects in mesendoderm specification and gastrulation (38–42). However, reduced Nodal signaling, either by introducing a hypomorphic allele into the null background (*Nodal*^{flax/-} or *Cripto*^{3flax/-} mice) or by mutating two components of the pathway (*Nodal*^{+/-}*Smad2*^{+/-} or *Nodal*^{+/-}*ActR2A*^{+/-}), results in mutant embryos that undergo gastrulation but exhibit the alobar HPE-like phenotype (39, 43–45). Further analysis of Nodal-insufficient embryos revealed that although

the mesendoderm is specified and gastrulation takes place, mesodermal cells fail to migrate anteriorly and form the PrCP (Figure 5A) (39, 43–45). Interestingly, physical ablation of the PrCP in amphibian or chicken embryos also causes cyclopia (46–48). Furthermore, transplantation of a donor PrCP laterally to that of the recipient PrCP activates expression of the ventral midline gene *NK2 homeobox 1* (*Nkx2.1*) and represses the expression of paired box gene 6 (*Pax6*), a marker for the dorsal telencephalon and eye field in the overlying neuroectoderm (49). These results indicate that the PrCP is required for eye field separation and forebrain patterning.

Nodal also collaborates with growth differentiation factor 1 (*Gdf1*), a member of the TGF- β superfamily that signals through the Nodal signaling pathway to regulate gastrulation and PrCP formation. Functional inactivation of *Gdf1* and genetic deletion of one Nodal allele (*Nodal*^{+/-}*Gdf1*^{+/-}) results in a defective PrCP and alobar HPE-like phenotype (50).



Table 1

Mouse models of HPE

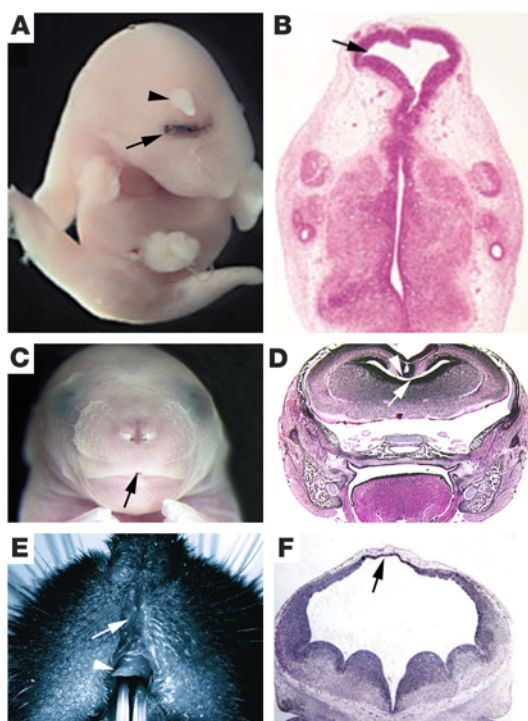
Phenotype	Gene/genotype	Related signaling pathway	Proposed mechanism	References
Alobar HPE-like phenotypes ^A	<i>Noda</i> ^{flox/-} , <i>Cripto3</i> ^{flox/-} , <i>Noda</i> ^{flox/-} <i>Smad2</i> ^{+/-} , <i>Noda</i> ^{flox/-} <i>ActR2A</i> ^{+/-} , <i>Noda</i> ^{flox/-} <i>Gdf1</i> ^{+/-}	Nodal signaling	PrCP defect	39, 43–45, 50
	<i>Chd</i> ^{+/-} <i>Nog</i> ^{+/-} , <i>Tsg</i> ^{+/-} ^B	Bmp signaling	PrCP defect	60, 61
	<i>Zic2</i> ^{ku/ku}	Nodal signaling?	PrCP defect	55
	<i>Shh</i> ^{+/-} , <i>Disp1</i> ^{+/-} , <i>Smo</i> ^{+/-}	Shh signaling	Loss of expression or function of Shh in the PrCP	66, 70, 71
	<i>Nog</i> ^{+/-} <i>Chd</i> ^{+/-}	Bmp signaling	Loss of expression or function of Shh in the PrCP	62
	<i>Otx2</i> ^{+/-} <i>Hnf3b</i> ^{+/-}		Loss of expression or function of Shh in the PrCP	74
	Semilobar HPE-like phenotypes ^C	<i>Six3</i> ^{+/-} ^B , <i>Six3</i> ^{+/-} ^{KiB} , <i>Six3</i> ^{+/-} <i>Shh</i> ^{+/-} ^B , <i>Six3</i> ^{+/-} ^{Ki} <i>Shh</i> ^{+/-} ^B , <i>Cdo</i> ^{+/-} ^B	Shh signaling	Defects of the 3 signaling centers along the midline of telencephalon
<i>Fgf8</i> ^{flox/flox} <i>Foxg1Cre</i> , <i>Fgfr1</i> ^{flox/flox} <i>Fgfr3</i> ^{+/-} <i>Foxg1Cre</i> , <i>Fgfr1</i> ^{flox/flox} <i>Fgfr2</i> ^{flox/flox} <i>Foxg1Cre</i> , <i>Fgf8</i> ^{-/neo}		Fgf signaling	Defects of the 3 signaling centers along the midline of telencephalon	82, 83
<i>Megalyn</i> ^{+/-} , <i>Tsg</i> ^{+/-} <i>Bmp4</i> ^{+/-}		Bmp signaling	Defects of the 3 signaling centers along the midline of telencephalon	63, 87, 88
Microforms of HPE ^D MIH-like phenotypes ^E		<i>Gas1</i> ^{+/-} , <i>Cdo</i> ^{+/-} , <i>Gli2</i> ^{+/-}	Shh signaling	Defective Shh signaling in FNP
	<i>Zic2</i> ^{kd/kd}		Defects in the dorsal signaling center of telencephalon	52
	<i>ShhN</i> ⁺	Ectopic Shh activity	Defects in the dorsal signaling center of telencephalon	101
	<i>ACTBCre</i> <i>Gdf7DTA</i>	Ablation of roof plate	Defects in the dorsal signaling center of telencephalon	99
	<i>Bmpr1a</i> ^{flox/flox} <i>Bmpr1b</i> ^{+/-} <i>Foxg1Cre</i>	Bmp signaling	Defects in the dorsal signaling	100
HPE-like phenotypes ^F	<i>Tgif</i> ^{Δexon3/Δexon3B}	Retinoic acid signaling? TGF-β signaling?		110
	<i>Cdc42</i> ^{+/-}		Loss of apical-basal polarity of the telencephalic neural epithelium	113

^AAlobar HPE-like phenotypes include single telencephalic vesicle, loss of MGE and most of LGE, and cyclopia. ^BMouse models that only exhibit HPE on the C57BL/6 background. ^CSemilobar HPE-like phenotypes include loss of septum, loss or hypoplasia of OB, loss of MGE, and midfacial defects. ^DMicroforms of HPE include midfacial defects. ^EMIH-like phenotypes include loss of dorsal midline structures of telencephalon. ^FHPE-like phenotypes include the presence of a single telencephalic vesicle due to abnormal folding of the neural epithelium or to failure in expansion and bifurcation of the cerebral hemispheres. Genes whose mutations have been identified in HPE patients are in bold. ACTB, actin, β; *ActR2A*, activin A receptor, type 2A; *Bmpr1a*, Bmp receptor, type 1a; *Cdc42*, cell division cycle 42 homolog; *Disp1*, dispatched homolog 1; DTA, diphtheria toxin A subunit; *fif*, *flox/flox*; FNP, frontonasal process; *Hnf3b*, hepatocyte nuclear factor 3β; OB, olfactory bulb; *Otx2*, orthodenticle homolog 2; *Smo*, smoothed homolog.

Zic2. The zinc finger protein *Zic2* shares sequence homology with Gli proteins and physically interacts with Gli2 (51). During gastrulation, *Zic2* is expressed in the mesoderm and head-fold region. At later stages, its expression is restricted to the dorsal neural tube and somites (52). *ZIC2* mutations account for 9.2% of all HPE cases (15). A missense mutation has been introduced into the fourth zinc finger domain of *Zic2* by ENU, which abolishes *Zic2*'s DNA binding and transcriptional activation abilities. Mouse embryos homozygous for this mutated *Zic2* allele (kumba [ku] allele) exhibit alobar HPE-like phenotype (53–55). Further studies revealed defects in the PrCP and anterior notochord of *Zic2*^{ku/ku} embryos (55). Interestingly, injection of an N-terminal truncated form of *zic2* that may function as a dominant negative leads to microcephaly (in which the circumference of the head is markedly smaller than average) and cyclopia in *Xenopus* embryos. Furthermore, depletion

of maternal *zic2*, resulting in the upregulation of Nodal signaling via the activation of *Xenopus* nodal-related (*xnr*) genes, leads to abnormal gastrulation and anterior truncation of the embryo (56). In mice, elevated Nodal signaling causes abnormal gastrulation; mesoderm cells arrest in/near the primitive streak and fail to move anteriorly (Figure 5A) (57). These studies raise interesting questions. Does *Zic2* regulate gastrulation via modulating Nodal activity in mice (Figure 5A)? Does increased Nodal activity cause HPE via abnormal gastrulation and PrCP defects?

Bone morphogenetic protein signaling pathway. Bone morphogenetic proteins (Bmps) belong to another branch of the TGF-β superfamily. They bind to type 1/2 Bmp receptors (BmpR1 and BmpR2) and signal through Smad1/5/8 and Smad4 complexes (Figure 4B) (58). Chordin (Chd) and noggin (Nog) act as secreted antagonists of Bmp. By directly interacting with Bmp ligands, these proteins are

**Figure 3**

Mouse models of HPE. (A and B) *Chd*^{-/-}*Nog*^{-/-} embryo exhibiting alobar HPE-like phenotype: cyclopia (arrow in A) and proboscis (arrowhead in A). (B) Coronal section of *Chd*^{-/-}*Nog*^{-/-} embryo highlighting the single cerebral ventricle (arrow). (C and D) *Six3*^{+/*ki*}*Shh*^{+/*+*} embryos exhibit semilobar HPE-like phenotype: agenesia of philtrum (arrow in C), lack of corpus callosum (arrowhead in D), and a single telencephalic ventricle anteriorly (arrow in D). (D) Coronal section of a *Six3*^{+/*ki*}*Shh*^{+/*+*} embryo. (E) Image of an adult *Cdo*^{-/-} mouse exhibiting microforms of HPE: dysgenesis of philtrum (arrow) and single central maxillary incisor (arrowhead). (F) Coronal section of an *ShhN*^{+/*+*} embryo exhibiting MIH-like phenotype: lack of dorsal telencephalic midline structures (arrow in F) and relatively normal ventral telencephalic structures. A and B are reprinted with permission from *Nature* (60); C and D are reprinted with permission from *Developmental Cell* (65); E is reprinted with permission from *Current Biology* (91); F is reprinted with permission from *Human Molecular Genetics* (101).

prevented from binding their receptors and activating downstream effectors (Figure 4B) (59). Twisted gastrulation (Tsg) is a secreted protein that directly interacts with Bmp and Chd (Figure 4B). The function of Tsg in regulating the Bmp signaling pathway is complex. On one hand, it behaves as a Bmp antagonist by promoting the formation of a stable Bmp/Chd/Tsg complex that prevents the binding of Bmps to their receptors (Figure 4B) (59). On the other, Tsg enhances Chd as a substrate for the metalloprotease tolloid, which cleaves Chd at specific sites. By promoting Chd degradation, Tsg releases Bmp from the inhibition of Chd and allows it to signal through its receptors (59). Therefore, Tsg promotes Bmp signaling in this setting (Figure 4B) (59). Although no mutations in Bmp signaling pathway components have been identified in patients with HPE, inactivation of *Chd* and *Nog* (*Chd*^{-/-}*Nog*^{-/-}) or *Tsg* (*Tsg*^{-/-}) causes PrCP defects and alobar HPE-like phenotype in mice (Figure 3, A and B) (60, 61). *Chd*, *Nog*, *Tsg*, and *Bmp7* are expressed in the axial mesoderm during gastrulation; thus, repression of Bmp sig-

naling activity is required for the normal development of the PrCP, and *Tsg* represses Bmp signaling (Figure 5A) (60–62). Interestingly, the alobar HPE-like phenotype reported in *Tsg*^{-/-} embryos can be observed only on the C57BL/6 background, suggesting that other genetic modifiers contribute to the phenotype (61, 63).

In summary, studies from genetic mouse models confirm the results obtained using ablation and transplantation experiments in several species and reveal that signaling from the PrCP is essential for the separation of the single eye field and the patterning and morphogenesis of the forebrain. Defects in the PrCP promote alobar HPE. This then led to the obvious question: What is the molecular identity of the PrCP signal?

Shh signaling pathway. One signal from the PrCP is Shh, a member of the Hedgehog family of secreted proteins. During early embryogenesis, *Shh* is expressed in the axial mesoderm, including the PrCP (64, 65). Beads soaked with Shh mimic the function of transplanted ectopic PrCP, i.e., they induce *Nkx2.1* expression and repress *Pax6* expression (49). In the *Shh*-null mouse forebrain, the most ventral structures are absent; the telencephalon fails to bifurcate, forming a single vesicle, and the eye field does not separate, thereby leading to cyclopia (66). These features are characteristic of alobar HPE and resemble the effects reported after physical ablation of the PrCP in chicken and amphibian embryos (46–48). These results demonstrate that Shh constitutes or contributes to the PrCP signal involved in the patterning of the forebrain (Figure 5A).

Shh signals through members of the Gli family of transcription factors. Gli1–3 are bifunctional transcriptional factors with repressor and activator domains that flank a central DNA-binding zinc finger region. In the absence of Shh signaling, Gli proteins are cleaved into truncated forms that function exclusively as transcriptional repressors (Figure 4C) (67, 68). Once Shh binds its receptor, patched (Ptch), and releases the serpentine protein smoothed (Smo) from the inhibition of Ptch, activated Smo prevents the cleavage of Gli. Unprocessed, full-length Gli accumulates in nuclei and activates downstream genes (Figure 4C) (67, 68). The secretion and long-range activity of Shh require the function of dispatched (Disp), a family of transmembrane proteins that shares sequence homology with and is structurally similar to Ptch (Figure 4C) (69). Mouse embryos null for *Disp1* or *Smo* exhibit a single telencephalic vesicle and cyclopia (70, 71).

Mutations in *SHH*, *GLI2*, *DISP1*, and *PTCH1* have been identified in HPE-affected individuals (14–16). Mutations in *SHH* alone account for 12.7% of HPE cases (15).

Similar to *Nog*^{-/-}*Chd*^{-/-} embryos, *Nog*^{+/-}*Chd*^{-/-} embryos exhibit alobar HPE and *Shh* expression in the PrCP is lost (62). *Chd*, *Nog*, *Bmp7*, and *Shh* are coexpressed in the PrCP, and ectopic Bmp activity represses *Shh* expression in mouse cephalic explants; thus, Bmp signaling may repress *Shh* expression in the PrCP (62). However, in *Nog*^{-/-}*Chd*^{-/-} embryos, excessive Bmp signaling also results in a defective PrCP (60); therefore, *Nog*^{+/-}*Chd*^{-/-} embryos should be stained with other PrCP markers to conclusively show that *Shh* expression in the PrCP, rather than the PrCP itself, is defective.

In mice, targeted deletion of the homeobox gene orthodenticle homolog 2 (*Otx2*) results in loss of the forebrain and midbrain (72), and deletion of the wing-helix hepatocyte nuclear factor 3 β (*Hnf3b*, also known as *Foxa2*) results in the absence of midline structures (axial mesoderm and floor plate) (73). Alobar HPE-like phenotype and loss of *Shh* expression in the ventral forebrain were observed in *Otx2*^{-/-}*Hnf3b*^{-/-} mouse embryos (74). Although *Shh* expression in the PrCP of earlier-stage mutant embryos was not reported by

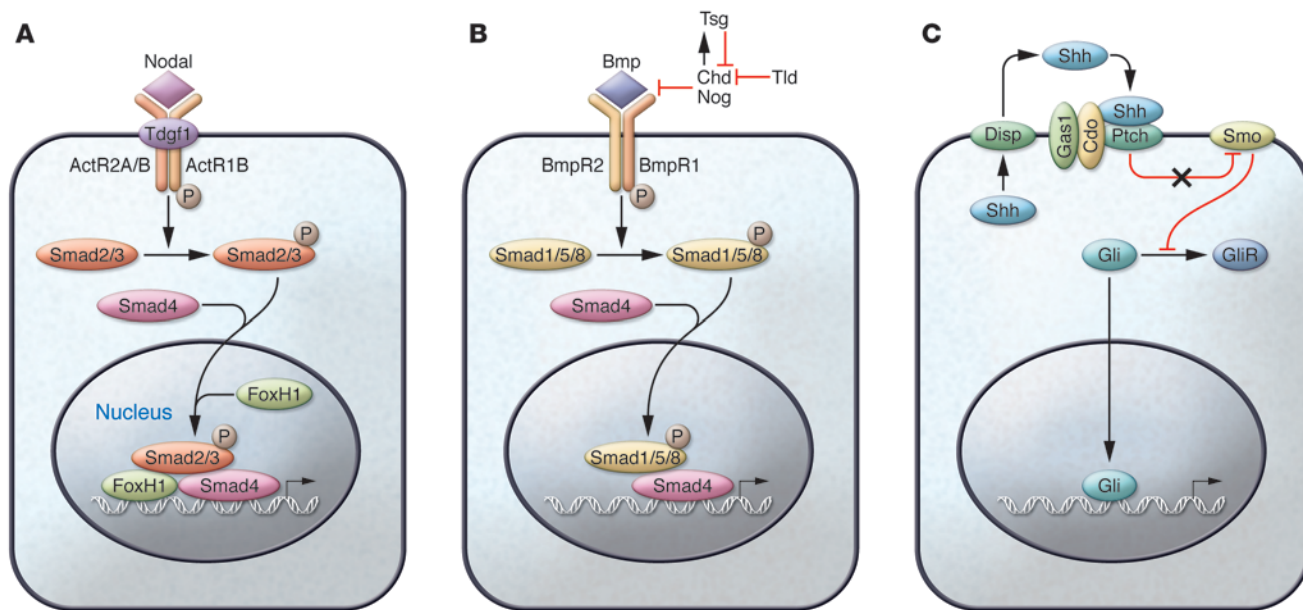


Figure 4 Signaling pathways involved in the pathogenesis of HPE. **(A)** Nodal signaling pathway. **(B)** Bmp signaling pathway. **(C)** Shh signaling pathway. ACTR2A, activin A receptor, type 2A; BMPR2, Bmp receptor 2; Disp, dispatched; Ptch, patched; Smo, smoothened; Tld, tollid.

the authors, based on the severity of the phenotype and the co-expression of *Otx2* and *Hnf3b* in the PrCP, it is likely that both genes coregulate *Shh* expression in the PrCP (Figure 5A).

In summary, detailed analyses of these mouse models of alobar HPE consistently demonstrate that *Shh* is the most important signaling molecule from the PrCP involved in the development of the forebrain and the pathogenesis of alobar HPE.

Mouse models exhibiting the semilobar HPE-like phenotype

Six3. During mouse embryogenesis, expression of the homeobox gene *Six3* starts as early as E7.0 in the ANE, which eventually gives rise to the telencephalon and eye field (65, 75). Around the 8-somite stage, *Six3* expression is restricted to the ventral forebrain and developing eyes. In patients with HPE, 46 mutations in *SIX3* have been identified and account for approximately 4% of HPE cases (15, 76).

Functional inactivation of *Six3* in mice causes the ectopic anterior expansion of wingless-related MMTV integration site 1 (*Wnt1*) expression and posteriorization of the mutant head (77, 78). As a consequence, the homozygous mutant heads lack the telencephalon and anterior diencephalon (77, 78). *Six3*^{-/-} mice appeared phenotypically normal in the outbred background used for these studies (77). However, HPE-like phenotypes were observed in approximately 16% of *Six3*^{+/-} embryos when backcrossed onto the inbred C57BL/6 background; this percentage increased to almost 85% in the third generation (65). Interestingly, 10% of *Six3* heterozygous embryos from a knockin mouse line (*Six3*^{+/ki}), generated by replacing WT *Six3* with the *Six3* mutant Six3V250A, which is identified in patients with HPE, exhibited a similar HPE-like phenotype in a mixed genetic background (65). Upon crossing this strain with *Shh*^{+/-} mice, 75% of the generated *Six3*^{+/ki}*Shh*^{+/-} embryos exhibited an HPE-like phenotype, and upon backcrossing into the C57BL/6 background, 100% exhibited HPE (Figure 3, C and D) (65).

Six3V250A has a valine-to-alanine substitution caused by a single nucleotide mutation (T749C) in the third helix of the homeodomain (21, 79). This amino acid substitution greatly reduced the DNA-binding ability of the mutant *Six3*, such that it behaved as a hypomorph (showing partial loss of gene function) (65, 79). These results demonstrated the hypomorphic nature of the HPE-promoting *Six3* mutations and uncovered the cooperation between *Six3* and *Shh* in the pathogenesis of HPE. Detailed phenotypic analysis of the HPE-like mutant embryos revealed the lack of the nasal septum, hypoplasia of the olfactory bulbs, and the presence of an anterior single telencephalic vesicle, resulting from the absence of the septum and the presence of two posteriorly separated cerebral hemispheres (65). All of these features resemble the characteristics typical of semilobar HPE.

Molecular marker analysis revealed the following ventral telencephalic defects: the presence of a single ganglionic eminence with molecular features of the lateral ganglionic eminence (LGE) and the presence of posterior dorsal telencephalic midline structures, such as hippocampus, cortical hem, and choroid plexus (65). Unlike the abnormal *Shh* expression observed in embryos exhibiting alobar HPE-like phenotype, *Shh* expression in the PrCP is not affected in embryos exhibiting semilobar HPE-like phenotype (65). However, *Shh* expression in the midline of the ventral forebrain (prospective hypothalamus) was missing (65). Interestingly, *Nkx2.1*, a marker for the prospective hypothalamus and a downstream target of *Shh* signaling from the PrCP, was still detected in these mutant embryos, suggesting that the absence of *Shh* expression in the ventral forebrain is not caused by a defective ANE (65). Further studies revealed that *Six3* is a direct activator of *Shh* expression in the ventral forebrain and, in turn, *Shh* maintains *Six3* expression in this region (Figure 5A) (65, 79).

Cell adhesion molecule-related/downregulated by oncogenes. Cell adhesion molecule-related/downregulated by oncogenes (*Cdo*) is a

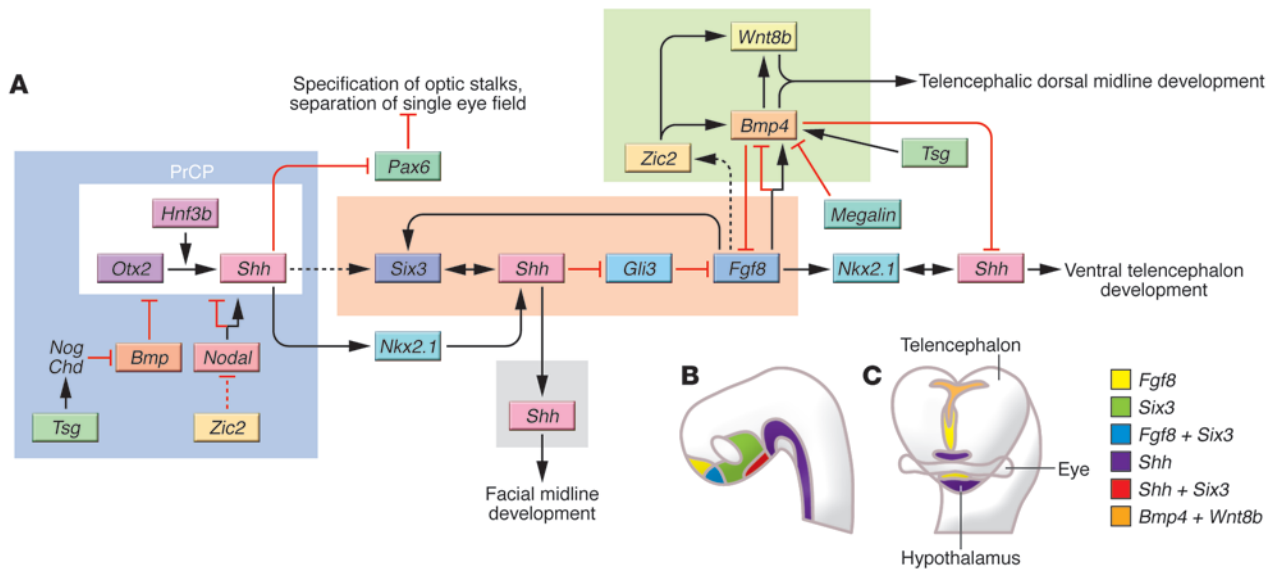


Figure 5

Mechanistic model of telencephalon development in normal and HPE conditions. **(A)** Model of normal mammalian telencephalic development. On the left side, the PrCP is represented by a white rectangle. The blue square around it highlights those steps known to be critical in the pathogenesis of alobar HPE. Toward the right side of the diagram, genes known to be important during subsequent steps of forebrain development are indicated. The orange rectangle highlights steps and genes important for semilobar HPE, the green rectangle highlights those important for MIH, and the gray rectangle highlights those important for microforms of HPE. Solid lines represent those processes that have been demonstrated and dashed lines represent those processes that have not yet been directly proved. To better understand the regional relationships between some of those critical genes, their normal expression patterns in the telencephalon at E9.0 and E10.5 are illustrated in **B** and **C**, respectively. **C** is adapted with permission from *Journal of Neuropathology and Experimental Neurology* (106). *Hnf3b*, hepatocyte nuclear factor 3 β ; *Otx2*, orthodenticle homolog 2; *Pax6*, paired box gene 6; *Wnt8b*, wingless-related MMTV integration site 8b.

member of the Ig superfamily and positively regulates *Shh* activity in vitro (80). A semilobar HPE-like phenotype has been observed in *Cdo*^{-/-} mouse embryos (80). As in *Six3* mutant embryos, *Shh* expression in the PrCP and *Nkx2.1* expression in the prospective hypothalamus of *Cdo*-null embryos was not affected; however, *Shh* expression in the prospective hypothalamus was lost (80). Results from the *Six3* and *Cdo* mouse models suggest that the loss of *Shh* expression in the ventral forebrain is the leading cause of semilobar HPE. However, in *Nkx2.1*-null embryos with normal *Shh* expression in the PrCP but absent *Shh* expression in the ventral forebrain, only ventral patterning defects occur (Figure 5A) (81). Therefore, the loss of *Shh* expression in the ventral forebrain is probably not sufficient to cause HPE (81).

Fgf signaling pathway. The semilobar HPE-like phenotype was reported in embryos with Fgf signaling reduced by the conditional deletion of *Fgf8* or Fgf receptors (Fgfrs) in the developing telencephalon (*Fgf8*^{flax/flax}*Foxg1Cre*, *Fgfr1*^{flax/flax}*Fgfr3*^{-/-}*Foxg1Cre*, and *Fgfr1*^{flax/flax}*Fgfr2*^{flax/flax}*Foxg1Cre*) or by the generation of the *Fgf8* hypomorphic allele *Fgf8*^{-/neo} (82, 83). During telencephalon development, several Fgf-encoding genes (*Fgf8*, *Fgf14*, *Fgf15*, *Fgf17*, and *Fgf18*) are expressed in the rostral midline of the telencephalon (commissural plate) and three Fgfr genes (*Fgfr1*, *Fgfr2*, and *Fgfr3*) are expressed in neural progenitor cells (83). In chicken embryos, ectopic *Fgf8* activity in the telencephalon frequently induces a sulcus (a depression or fissure in the brain surface) that resembles an ectopic rostral midline (84). Consistent with these results, reduced Fgf signaling in mouse embryos prevents the separation of the anterior cerebral hemispheres (82, 83). In the ventral telencephalon, the defects are similar to those observed in *Six3*-promoted

HPE (i.e., loss of median ganglionic eminence [MGE] and presence of a single ganglionic eminence with LGE identity) (82).

Fgf8 expression is downregulated in the commissural plate of *Shh*-null embryos (85). This finding supports the hypothesis that *Fgf8* functions downstream of *Shh* during telencephalon patterning. However, the source of *Shh* activity required for maintaining *Fgf8* expression in the commissural plate is unknown. Is the *Shh* signaling activity from the PrCP or the ventral forebrain? *Fgf8* expression in *Shh*-null embryos is downregulated after the 10-somite stage, shortly after the normal initiation of *Shh* expression in the ventral forebrain; thus, the ventral forebrain may be the source of *Shh* that maintains *Fgf8* expression in the commissural plate. Further support of this hypothesis is provided by the fact that *Fgf8* expression is downregulated after the 10-somite stage in the commissural plate of *Six3*-haploinsufficient or *Cdo*-null embryos, in which *Shh* expression is absent from the ventral forebrain but remains normal in the PrCP (65, 80). Interestingly, *Fgf8* expression in the commissural plate is restored in *Shh**Gli3* double-null embryos, in which the MGE and LGE are rescued (86). However, deletion of *Gli3* could not rescue the ventral telencephalic defects resulting from reduced Fgf signaling (83). These results suggest that Fgf signaling functions downstream of *Shh* signaling activity in the regulation of ventral telencephalic patterning (Figure 5A).

Megalyn. Megalyn is a member of the LDL receptor-related protein family (87). *Megalyn* (also known as *Lrp2*) is expressed in the yolk sac and the apical side of the neuroepithelium of early embryos, and its functional inactivation causes semilobar HPE-like phenotypes (87, 88). Megalyn is an endocytic receptor that binds to the amino-terminal of *Shh* and internalizes it; thus, Megalyn may



regulate the Shh signaling pathway (89, 90), and inactivation of *Megalyn* may cause HPE by affecting Shh signaling. Megalyn is also an endocytic receptor for Bmp4 and negatively regulates Bmp4 activity (Figure 5A) (88). Loss of *Megalyn* leads to an increase in Bmp4 expression and signaling in the dorsal telencephalon of mutant embryos and the subsequent loss of *Shh* expression in the ventral telencephalon, which ultimately leads to HPE (88). Ectopic Bmp4 activity in the ventral telencephalon downregulates *Shh* and causes HPE in chicken embryos (84). Interestingly, reducing Bmp signaling by deleting one copy of *Bmp4* in a *Tsg*-null background in the B6SJL/F1 strain also causes the loss of *Shh* expression in the ventral forebrain and that of *Fgf8* in the commissural plate (Figure 5A). These alterations ultimately lead to the semilobar HPE-like phenotype (63). The fact that this phenotype is observed only in *Tsg*^{-/-} embryos upon deleting a *Bmp4* allele supports the argument that during telencephalon patterning and morphogenesis Tsg functions as an agonist of Bmp signaling (Figure 5A) (63). These results suggest that excessive or insufficient Bmp signaling causes similar telencephalic defects.

Mouse models of lobar HPE

No mouse models of lobar HPE have yet been reported, probably because the relatively mild forebrain defects defining this alteration can be easily overlooked. A more detailed and thorough analysis of the generated mouse models will be required to uncover these phenotypic alterations.

Mouse models exhibiting microform HPE

The pathologic variability of HPE includes milder forms of the disease, such as microforms, in which affected individuals exhibit a normal brain but have mild facial midline defects.

Cdo. As mentioned above, *Cdo*-null mouse embryos exhibit semilobar HPE in the C57BL/6 background (80). However, in a mixed 129/Sv/C57BL/6 background, *Cdo*-null pups exhibit no malformation of the forebrain but mild facial defects reminiscent of those in patients with microform HPE. These include craniofacial defects, dysgenesis of the philtrum (the vertical groove in the upper lip), lack or hypoplasia of the cartilage of the nasal septum, and a lack of primary palate (Figure 3E) (91). During facial development, cranial neural crest cells migrate from the dorsal midline of the posterior diencephalon to form several facial primordia, including the frontonasal process (FNP). The FNP later splits at the midline into 2 medial nasal processes that fuse to form the nasal septum, philtrum, premaxilla, upper incisors, and primary palate (92). *Shh* is expressed in the facial ectoderm of the FNP, and Shh signaling is important for normal development of the facial midline (93, 94). *Cdo* is also highly expressed in the FNP and, as mentioned above, it positively regulates Shh activity. These results suggest that *Cdo* may regulate facial midline development by modulating Shh signaling (80, 91).

Growth arrest-specific 1. Microform HPE has been described in mice lacking the activity of the growth arrest-specific 1 (*Gas1*) gene (95). In certain genetic backgrounds, these mice exhibit midfacial hypoplasia, solitary central maxillary incisors, and cleft palate (95). *Gas1* encodes a membrane glycoprotein, and like *Cdo*, it functions as an agonist of Shh signaling during facial midline development (95, 96). In addition, *Gas1* and *Cdo* cooperate to promote Shh signaling during neural tube patterning and craniofacial and vertebrae development (96). Although *Gas1* and *Cdo* have similar, cooperative functions during neural and craniofacial development, whether *Gas1*-null or *Gas1/Cdo* double-heterozygous

embryos phenocopy *Cdo*-null embryos and exhibit semilobar HPE in a C57BL/6 background remains unknown.

Gli2. As previously mentioned, *Gli2* is a component of the Shh signaling pathway, and mutations in *GLI2* have been identified in patients with HPE (14–16, 67, 68). However, functional inactivation of *Gli2* in mice causes only mild defects (e.g., variable loss of pituitary and lack or partial fusion of the maxillary central incisors) (97, 98). *Gli2* inactivation downregulates *Gli1* and *Ptch1* from the epithelium of the tooth germ, a result suggesting that reduced Shh signaling contributes to the defects observed in the maxillary central incisors (98).

Mouse models exhibiting MIH

Patients with MIH generally lack the craniofacial and ventral telencephalic defects normally associated with HPE (22, 23). *ZIC2* is the only gene whose mutations have been identified in patients with MIH (24). As mentioned above, removal of *Zic2* activity causes alobar HPE in mice (55). However, reduced *Zic2* results in normal telencephalic patterning and craniofacial development but a defective telencephalon roof plate that affects the separation of the cerebral hemispheres (Figure 5A) (52). These phenotypes are some of the key features of MIH. Ablation of the roof plate or telencephalic deletion of Bmp receptors also causes dorsal telencephalic midline defects and MIH-like phenotypes (99, 100). Similar MIH-like phenotypes have been observed in *ShhN*^{+/+} embryos in which expression of noncholesterol-modified Shh is ectopically expanded into the dorsal telencephalon (Figure 3F) (101). This ectopic activity upregulates *Fgf8* expression in the commissural plate and downregulates that of *Bmp* and *Wnt* genes in the roof plate (101). As a consequence, the roof plate fails to invaginate, and dorsal midline structures fail to develop (101). Results from these mouse models highlight the critical role of roof plate-derived Bmp and Wnt signaling activity in the pathogenesis of MIH.

Clinical implications

The knowledge we have gained from the animal models of HPE described in this Review has significantly improved our understanding of normal telencephalic development and the pathogenesis and clinical variability of HPE. This understanding should foster better tools for genetic screening for HPE and, therefore, improve the prevention, diagnosis, and treatment of patients with HPE.

Mechanistic model of telencephalon development in normal and HPE conditions

To better interpret the pathogenesis and phenotypic variability of HPE, we have now incorporated into the current model of normal telencephalic development, data generated from the analysis of animal models of HPE (Figure 5). The current view indicates that starting at pre-gastrula stages, Nodal activity regulates the formation of the primitive streak (Figure 5A) (2, 38, 57). Upon the initiation of gastrulation, the development and maintenance of the PrCP and anterior notochord requires the activity of Bmp signaling antagonists such as *Nog*, *Chd* and *Tsg* (Figure 5A) (60). Toward the end of gastrulation, the Shh-expressing axial mesoderm is formed along the midline of mouse embryos (10). Then Shh signaling originating in the PrCP acts on the overlying ANE to separate the single eye field, induce optic stalk specification, and activate downstream genes such as *Nkx2.1* and probably *Six3* in the midline of the ventral forebrain (Figure 5A) (66, 102).

Next, the developing forebrain becomes patterned along the ventrodorsal and anteroposterior axes. On the ventral side, *Six3*



and *Nkx2.1* are required to activate *Shh* expression in the ventral forebrain (65, 79, 81) (Figure 5, A and B). In this region and by antagonizing the repressor activity of *Gli3*, *Shh* activity maintains *Fgf8* expression in the commissural plate (Figure 5, A and B) (85, 86). In turn, *Fgf8* activates *Nkx2.1* expression in the ventral telencephalon, which in turn, induces *Shh* expression and specifies the MGE fate (Figure 5A) (65, 81, 82, 103).

In the dorsal telencephalon, *Fgf8* activity restricts *Wnt8b* to the dorsal midline and regulates *Bmp4* expression in a dosage-dependent manner (Figure 5, A and C) (82, 104). *Bmp4* activity also appears necessary to restrict *Fgf8* and *Shh* expression (63, 85). In addition and as shown in telencephalic explants maintained in culture, *Fgf8* appears to regulate *Zic2* expression in the dorsal midline (105). As mentioned above, *Zic2* activity is necessary for the development of the telencephalic dorsal midline (Figure 5A) (52). Thus, by maintaining *Fgf8* expression in the commissural plate, *Shh* regulates the development of dorsal midline structures. *Shh*, *Fgf*, *Bmp*, and *Wnt* signaling pathways regulate each other and work synergistically to regulate the regional specification and morphogenesis of the telencephalon (9, 84, 85, 106) (Figure 5). Work performed in chicken embryos suggests that *Shh* signal from the ventral telencephalon activates its own expression in the facial ectoderm, in which *Shh* activity is crucial for facial midline development (Figure 5A) (93, 94, 107).

Temporal or spatial alterations in cellular or molecular processes essential for normal forebrain development could lead to different types of HPE. Alterations occurring during early stages (gastrulation and head fold, E6.5–8.5 in mice; Carnegie Stage 7–9 [CS7–9] in humans) that might affect the PrCP or disrupt *Shh* expression are most likely to promote alobar HPE (Figure 5A). Alterations occurring during or after the closure of the neural tube (E8.5–10.5 in mice; CS10–14 in humans) disturb rostral (*Fgf8*) and ventral (*Shh*) telencephalic patterning centers, thereby impairing ventral specification and rostral midline development and causing semilobar HPE (Figure 5A).

In MIH, the dorsal telencephalic patterning center is defective (*Bmp* and *Wnt*), i.e., dorsal midline structures fail to develop but do not affect dorsoventral patterning of the telencephalon (Figure 5A). In microform HPE, *Shh* signaling is impaired in the facial ectoderm; therefore, facial midline structures develop abnormally but forebrain development is not affected (Figure 5A).

Variable pathology of HPE

The clinical manifestation of HPE is highly variable; the whole spectrum of HPE is observed in family members carrying the same mutation (16). The explanation for this variability is the multi-hit model: HPE is not a monogenic disease; more than two genetic and/or environmental factors contribute to its phenotype (108). Studies from mouse models of HPE support this model. For example, deletion of one *Nodal* allele does not cause HPE; however, upon the additional deletion of one or two copies of another gene in the same signaling pathway (e.g., *Nodal*^{-/-}*Smad2*^{-/-} or *Nodal*^{-/-}*ActR2A*^{-/-}), *Nodal* signaling becomes haploinsufficient, and the mutant embryos exhibit HPE (39, 45). Similarly, when two genes that function redundantly or synergistically are simultaneously deleted (e.g., *Nodal*^{-/-}*Gdf1*^{-/-}, *Chd*^{-/-}*Nog*^{-/-}, *Chd*^{-/-}*Nog*^{+/-}, *Tsg*^{-/-}*Bmp4*^{+/-}, or *Otx2*^{+/-}*Hnf3b*^{+/-}), HPE arises (50, 60, 62, 63, 74).

Unidentified genetic modifiers associated with different mouse strains contribute to the pathogenesis of HPE. For instance, *Tsg*^{-/-}, *Six3*^{+/-}, *Six3*^{+/ki}, or *Six3*^{+/ki}*Shh*^{+/-} embryos exhibit HPE only

on a C57BL/6 background (61, 65). Similarly, in a mixed 129/Sv/C57BL/6 background, *Cdo*-null embryos exhibit microform HPE; however, upon backcrossing onto the C57BL/6 background, they exhibit semilobar HPE (80, 91). Mutations in the atypical homeodomain-containing transcription factor TGIF have been identified in patients with HPE (13–16); however, removal of the third exon of *Tgfi* in mice results in various brain defects, including HPE, only in the C57BL/6 background (109, 110).

Consistent with the multi-hit model, mutations in two different HPE-associated genes, *SHH* and *TGIF*, have been identified in some patients with HPE (108). Considering the growing list of HPE-associated genes, it will not be surprising to identify many patients carrying more than one mutated gene.

Forebrain-specific defects associated with HPE

Except for those individuals with syndromic disease (e.g., Smith-Lemli-Opitz syndrome), most patients with HPE exhibit forebrain malformations only; no defects occur in any other organ. HPE is an autosomal-dominant disease in humans; however, most mouse models of HPE are autosomal recessive. One possible explanation for the forebrain-specific phenotype is that HPE is not monogenic, and another factor(s) contributing to the phenotype specifically affects the expression or function of HPE-associated genes in the forebrain. For example, *Shh*-null mouse embryos exhibit the alobar HPE-like phenotype and defects in other organs whose development requires *Shh* signaling (66). However, removal of one copy of *Shh* causes semilobar HPE only if a copy of *Six3* is also deleted (65).

Another explanation for the forebrain-specific phenotype is that HPE-promoting mutations occur in the regulatory regions driving the expression of HPE-associated genes in the forebrain. Although no mouse models of HPE addressing this possibility have been generated, mutations in a conserved regulatory element of *SHH* have been identified in a patient with semilobar HPE (79). It will be interesting to determine whether deletion of this conserved regulatory element in mice will also result in semilobar HPE.

Finally, the forebrain may be more sensitive to changes in the activity of HPE-associated genes. For instance, *Shh* signaling is essential for forebrain and limb development, and its positive regulator, *Cdo*, is expressed along the neural tube and in developing limbs. However, *Cdo*-null embryos exhibit semilobar HPE without limb defects (80). Within the forebrain, some developmental processes are more sensitive to gene dosage than others. For example, at the head-fold stage, *Six3* is expressed in the ANE and is responsible for maintaining anterior neural identity. Removal of one *Six3* allele does not affect anteroposterior patterning of the neural tube; however, dorsoventral patterning of the telencephalon is impaired and HPE arises (65). This result argues that dorsoventral patterning of the telencephalon is more sensitive to *Six3* dosage than is the specification of the telencephalon.

Screening for HPE-associated mutations

The identified HPE-associated genes have been related to two signaling pathways, *Nodal* and *Shh*; however, these mutations account for only about 28% of all HPE cases. As most sequence analyses are focused on the coding regions of candidate genes, mutations in the regulatory regions that may downregulate the expression of the gene are bound to be overlooked. Therefore, the actual percentage of mutations in any identified gene could be higher. However, other HPE-associated genes eventually may be identified. Studies of animal models of HPE have identified some



putative candidates (e.g., genes related to Bmp and Fgf signaling pathways). As discussed above, HPE is not a monogenic disease; therefore, single mutations identified in patients with HPE may not be enough to cause the phenotype. Therefore, identification of new HPE-associated genes is crucial for accurate molecular diagnosis and further understanding of the pathogenesis of HPE.

Acknowledgments

We thank L. Solnica-Krezel, R.S. Srinivasan, A. Lavado, and A. Inbal for critical reading of this manuscript and A. McArthur

for editing the manuscript. This project was supported in part by NIH grant R01 NS052386 and Cancer Center Support grant CA-21765 (to G. Oliver) and the American Lebanese Syrian Associated Charities (ALSAC).

Address correspondence to: Guillermo Oliver, Department of Genetics and Tumor Cell Biology, St. Jude Children’s Research Hospital, Memphis, Tennessee 38105, USA. Phone: (901) 595-2697; Fax: (901) 595-6035; E-mail: guillermo.oliver@stjude.org.

1. Robb, L., and Tam, P.P. 2004. Gastrula organiser and embryonic patterning in the mouse. *Semin. Cell Dev. Biol.* **15**:543–554.
2. Tam, P.P., and Loebel, D.A. 2007. Gene function in mouse embryogenesis: get set for gastrulation. *Nat. Rev. Genet.* **8**:368–381.
3. Wilson, S.W., and Houart, C. 2004. Early steps in the development of the forebrain. *Dev. Cell.* **6**:167–181.
4. Rallu, M., Corbin, J.G., and Fishell, G. 2002. Parsing the prosencephalon. *Nat. Rev. Neurosci.* **3**:943–951.
5. Levine, A.J., and Brivanlou, A.H. 2007. Proposal of a model of mammalian neural induction. *Dev. Biol.* **308**:247–256.
6. Stern, C.D. 2004. *Gastrulation: from cells to embryo*. Cold Spring Harbor Laboratory Press. Cold Spring Harbor, New York, USA. 731 pp.
7. Knoetgen, H., Viebahn, C., and Kessel, M. 1999. Head induction in the chick by primitive endoderm of mammalian, but not avian origin. *Development.* **126**:815–825.
8. Monuki, E.S., and Walsh, C.A. 2001. Mechanisms of cerebral cortical patterning in mice and humans. *Nat. Neurosci.* **4**(Suppl.):1199–1206.
9. Sur, M., and Rubenstein, J.L. 2005. Patterning and plasticity of the cerebral cortex. *Science.* **310**:805–810.
10. Rubenstein, J.L., and Beachy, P.A. 1998. Patterning of the embryonic forebrain. *Curr. Opin. Neurobiol.* **8**:18–26.
11. Wilson, S.W., and Rubenstein, J.L. 2000. Induction and dorsoventral patterning of the telencephalon. *Neuron.* **28**:641–651.
12. DeMyer, W.E. 1977. Holoprosencephaly (cyclopiarhinencephaly). In *Handbook of clinical neurology*. P.J. Vinken and G.W. Bruyn, editors. North-Holland Publishing Company. Amsterdam, The Netherlands. 431–478.
13. Muenke, M., and Cohen, M.M., Jr. 2000. Genetic approaches to understanding brain development: holoprosencephaly as a model. *Ment. Retard. Dev. Disabil. Res. Rev.* **6**:15–21.
14. Cohen, M.M., Jr. 2006. Holoprosencephaly: clinical, anatomic, and molecular dimensions. *Birth Defects Res. Part A Clin. Mol. Teratol.* **76**:658–673.
15. Dubourg, C., et al. 2007. Holoprosencephaly. *Orphanet J. Rare Dis.* **2**:8.
16. Krauss, R.S. 2007. Holoprosencephaly: new models, new insights. *Expert Rev. Mol. Med.* **9**:1–17.
17. Takahashi, T., et al. 2003. Semilobar holoprosencephaly with midline ‘seam’: a topologic and morphogenetic model based upon MRI analysis. *Cereb. Cortex.* **13**:1299–1312.
18. Ribeiro, L.A., El-Jaick, K.B., Muenke, M., and Richieri-Costa, A. 2006. SIX3 mutations with holoprosencephaly. *Am. J. Med. Genet. A.* **140**:2577–2583.
19. Schell, U., et al. 1996. Molecular characterization of breakpoints in patients with holoprosencephaly and definition of the HPE2 critical region 2p21. *Hum. Mol. Genet.* **5**:223–229.
20. Nanni, L., et al. 1999. The mutational spectrum of the sonic hedgehog gene in holoprosencephaly: SHH mutations cause a significant proportion of autosomal dominant holoprosencephaly. *Hum. Mol. Genet.* **8**:2479–2488.
21. Wallis, D.E., et al. 1999. Mutations in the homeodomain of the human SIX3 gene cause holoprosencephaly. *Nat. Genet.* **22**:196–198.
22. Lewis, A.J., et al. 2002. Middle interhemispheric variant of holoprosencephaly: a distinct cliniconororadiologic subtype. *Neurology.* **59**:1860–1865.
23. Simon, E.M., et al. 2002. The middle interhemispheric variant of holoprosencephaly. *AJNR Am. J. Neuroradiol.* **23**:151–156.
24. Brown, L.Y., et al. 2001. Holoprosencephaly due to mutations in ZIC2: alanine tract expansion mutations may be caused by parental somatic recombination. *Hum. Mol. Genet.* **10**:791–796.
25. Cohen, M.M., Jr., and Shiota, K. 2002. Teratogenesis of holoprosencephaly. *Am. J. Med. Genet.* **109**:1–15.
26. Hayhurst, M., and McConnell, S.K. 2003. Mouse models of holoprosencephaly. *Curr. Opin. Neurol.* **16**:135–141.
27. Muenke, M., and Beachy, P.A. 2000. Genetics of ventral forebrain development and holoprosencephaly. *Curr. Opin. Genet. Dev.* **10**:262–269.
28. Roessler, E., et al. 2009. The full spectrum of holoprosencephaly-associated mutations within the ZIC2 gene in humans predicts loss-of-function as the predominant disease mechanism. *Hum. Mutat.* **30**:E541–E554.
29. Kolf-Clauw, M., et al. 1996. Inhibition of 7-dehydrocholesterol reductase by the teratogen AY9944: a rat model for Smith-Lemli-Opitz syndrome. *Teratology.* **54**:115–125.
30. Gofflot, F., Kolf-Clauw, M., Clotman, F., Roux, C., and Picard, J.J. 1999. Absence of ventral cell populations in the developing brain in a rat model of the Smith-Lemli-Opitz syndrome. *Am. J. Med. Genet.* **87**:207–216.
31. Aoto, K., Shikata, Y., Higashiyama, D., Shiota, K., and Motoyama, J. 2008. Fetal ethanol exposure activates protein kinase A and impairs Shh expression in prechordal mesendoderm cells in the pathogenesis of holoprosencephaly. *Birth Defects Res. A Clin. Mol. Teratol.* **82**:224–231.
32. Higashiyama, D., et al. 2007. Sequential developmental changes in holoprosencephalic mouse embryos exposed to ethanol during the gastrulation period. *Birth Defects Res. A Clin. Mol. Teratol.* **79**:513–523.
33. Nagase, T., et al. 2005. Craniofacial anomalies of the cultured mouse embryo induced by inhibition of sonic hedgehog signaling: an animal model of holoprosencephaly. *J. Craniofac. Surg.* **16**:80–88.
34. Shen, M.M. 2007. Nodal signaling: developmental roles and regulation. *Development.* **134**:1023–1034.
35. Gritsman, K., et al. 1999. The EGF-CFC protein one-eyed pinhead is essential for nodal signaling. *Cell.* **97**:121–132.
36. Sampath, K., et al. 1998. Induction of the zebrafish ventral brain and floorplate requires cyclops/nodal signalling. *Nature.* **395**:185–189.
37. Rebagliati, M.R., Toyama, R., Haffter, P., and Dawid, I.B. 1998. cyclops encodes a nodal-related factor involved in midline signaling. *Proc. Natl. Acad. Sci. U. S. A.* **95**:9932–9937.
38. Zhou, X., Sasaki, H., Lowe, L., Hogan, B.L., and Kuehn, M.R. 1993. Nodal is a novel TGF-beta-like gene expressed in the mouse node during gastrulation. *Nature.* **361**:543–547.
39. Nomura, M., and Li, E. 1998. Smad2 role in mesoderm formation, left-right patterning and craniofacial development. *Nature.* **393**:786–790.
40. Ding, J., et al. 1998. Cripto is required for correct orientation of the anterior-posterior axis in the mouse embryo. *Nature.* **395**:702–707.
41. Yamamoto, M., et al. 2001. The transcription factor FoxH1 (FAST) mediates Nodal signaling during anterior-posterior patterning and node formation in the mouse. *Genes Dev.* **15**:1242–1256.
42. Hoodless, P.A., et al. 2001. FoxH1 (Fast) functions to specify the anterior primitive streak in the mouse. *Genes Dev.* **15**:1257–1271.
43. Lowe, L.A., Yamada, S., and Kuehn, M.R. 2001. Genetic dissection of nodal function in patterning the mouse embryo. *Development.* **128**:1831–1843.
44. Chu, J., et al. 2005. Non-cell-autonomous role for Cripto in axial midline formation during vertebrate embryogenesis. *Development.* **132**:5539–5551.
45. Song, J., et al. 1999. The type II activin receptors are essential for egg cylinder growth, gastrulation, and rostral head development in mice. *Dev. Biol.* **213**:157–169.
46. Adelmann, H.B. 1936. The problem of cyclopia. Pt. II. *Q. Rev. Biol.* **11**:284–304.
47. Li, H., Tierney, C., Wen, L., Wu, J.Y., and Rao, Y. 1997. A single morphogenetic field gives rise to two retina primordia under the influence of the prechordal plate. *Development.* **124**:603–615.
48. Pera, E.M., and Kessel, M. 1997. Patterning of the chick forebrain anlage by the prechordal plate. *Development.* **124**:4153–4162.
49. Shimamura, K., and Rubenstein, J.L. 1997. Inductive interactions direct early regionalization of the mouse forebrain. *Development.* **124**:2709–2718.
50. Andersson, O., Reissmann, E., Jornvall, H., and Ibanez, C.F. 2006. Synergistic interaction between Gdf1 and Nodal during anterior axis development. *Dev. Biol.* **293**:370–381.
51. Koyabu, Y., Nakata, K., Mizugishi, K., Aruga, J., and Mikoshiba, K. 2001. Physical and functional interactions between Zic and Gli proteins. *J. Biol. Chem.* **276**:6889–6892.
52. Nagai, T., et al. 2000. Zic2 regulates the kinetics of neurulation. *Proc. Natl. Acad. Sci. U. S. A.* **97**:1618–1623.
53. Brown, L., Paraso, M., Arkell, R., and Brown, S. 2005. In vitro analysis of partial loss-of-function ZIC2 mutations in holoprosencephaly: alanine tract expansion modulates DNA binding and transactivation. *Hum. Mol. Genet.* **14**:411–420.
54. Elms, P., Siggers, P., Napper, D., Greenfield, A., and Arkell, R. 2003. Zic2 is required for neural crest formation and hindbrain patterning during mouse development. *Dev. Biol.* **264**:391–406.
55. Warr, N., et al. 2008. Zic2-associated holoprosencephaly is caused by a transient defect in the organizer region during gastrulation. *Hum. Mol. Genet.* **17**:2986–2996.
56. Houston, D.W., and Wylie, C. 2005. Maternal Xenopus Zic2 negatively regulates Nodal-related gene expression during anteroposterior patterning. *Development.* **132**:4845–4855.
57. Iratni, R., et al. 2002. Inhibition of excess nodal sig-



- naling during mouse gastrulation by the transcriptional corepressor DRAP1. *Science*. **298**:1996–1999.
58. Shi, Y., and Massague, J. 2003. Mechanisms of TGF-beta signaling from cell membrane to the nucleus. *Cell*. **113**:685–700.
59. De Robertis, E.M., and Kuroda, H. 2004. Dorsal-ventral patterning and neural induction in *Xenopus* embryos. *Annu. Rev. Cell Dev. Biol.* **20**:285–308.
60. Bachiller, D., et al. 2000. The organizer factors Chordin and Noggin are required for mouse forebrain development. *Nature*. **403**:658–661.
61. Petryk, A., et al. 2004. The mammalian twisted gastrulation gene functions in foregut and craniofacial development. *Dev. Biol.* **267**:374–386.
62. Anderson, R.M., Lawrence, A.R., Stottmann, R.W., Bachiller, D., and Klingensmith, J. 2002. Chordin and noggin promote organizing centers of forebrain development in the mouse. *Development*. **129**:4975–4987.
63. Zakin, L., and De Robertis, E.M. 2004. Inactivation of mouse Twisted gastrulation reveals its role in promoting Bmp4 activity during forebrain development. *Development*. **131**:413–424.
64. Shimamura, K., Hartigan, D.J., Martinez, S., Puelles, L., and Rubenstein, J.L. 1995. Longitudinal organization of the anterior neural plate and neural tube. *Development*. **121**:3923–3933.
65. Geng, X., et al. 2008. Haploinsufficiency of Six3 fails to activate Sonic hedgehog expression in the ventral forebrain and causes holoprosencephaly. *Dev. Cell*. **15**:236–247.
66. Chiang, C., et al. 1996. Cyclopia and defective axial patterning in mice lacking Sonic hedgehog gene function. *Nature*. **383**:407–413.
67. Cohen, M.M., Jr. 2003. The hedgehog signaling network. *Am. J. Med. Genet. A*. **123A**:5–28.
68. Ingham, P.W., and Placzek, M. 2006. Orchestrating ontogenesis: variations on a theme by sonic hedgehog. *Nat. Rev. Genet.* **7**:841–850.
69. Burke, R., et al. 1999. Dispatched, a novel sterol-sensing domain protein dedicated to the release of cholesterol-modified hedgehog from signaling cells. *Cell*. **99**:803–815.
70. Ma, Y., et al. 2002. Hedgehog-mediated patterning of the mammalian embryo requires transporter-like function of dispatched. *Cell*. **111**:63–75.
71. Zhang, X.M., Ramalho-Santos, M., and McMahon, A.P. 2001. Smoothed mutants reveal redundant roles for Shh and Ihh signaling including regulation of L/R symmetry by the mouse node. *Cell*. **106**:781–792.
72. Matsuo, I., Kuratani, S., Kimura, C., Takeda, N., and Aizawa, S. 1995. Mouse Otx2 functions in the formation and patterning of rostral head. *Genes Dev*. **9**:2646–2658.
73. Ang, S.L., and Rossant, J. 1994. HNF-3 beta is essential for node and notochord formation in mouse development. *Cell*. **78**:561–574.
74. Jin, O., Harpal, K., Ang, S.L., and Rossant, J. 2001. Otx2 and HNF3beta genetically interact in anterior patterning. *Int. J. Dev. Biol.* **45**:357–365.
75. Oliver, G., et al. 1995. Six3, a murine homologue of the sine oculis gene, demarcates the most anterior border of the developing neural plate and is expressed during eye development. *Development*. **121**:4045–4055.
76. Domene, S., et al. 2008. Mutations in the human SIX3 gene in holoprosencephaly are loss-of-function. *Hum. Mol. Genet.* **17**:3919–3928.
77. Lagutin, O.V., et al. 2003. Six3 repression of Wnt signaling in the anterior neuroectoderm is essential for vertebrate forebrain development. *Genes Dev*. **17**:368–379.
78. Lavado, A., Lagutin, O.V., and Oliver, G. 2008. Six3 inactivation causes progressive caudalization and aberrant patterning of the mammalian diencephalon. *Development*. **135**:441–450.
79. Jeong, Y., et al. 2008. Regulation of a remote Shh forebrain enhancer by the Six3 homeoprotein. *Nat. Genet.* **40**:1348–1353.
80. Zhang, W., Kang, J.S., Cole, F., Yi, M.J., and Krauss, R.S. 2006. Cdo functions at multiple points in the Sonic Hedgehog pathway, and Cdo-deficient mice accurately model human holoprosencephaly. *Dev. Cell*. **10**:657–665.
81. Sussel, L., Marin, O., Kimura, S., and Rubenstein, J.L. 1999. Loss of Nkx2.1 homeobox gene function results in a ventral to dorsal molecular respecification within the basal telencephalon: evidence for a transformation of the pallidum into the striatum. *Development*. **126**:3359–3370.
82. Storm, E.E., et al. 2006. Dose-dependent functions of Fgf8 in regulating telencephalic patterning centers. *Development*. **133**:1831–1844.
83. Gutin, G., et al. 2006. FGF signalling generates ventral telencephalic cells independently of SHH. *Development*. **133**:2937–2946.
84. Crossley, P.H., Martinez, S., Ohkubo, Y., and Rubenstein, J.L. 2001. Coordinate expression of Fgf8, Otx2, Bmp4, and Shh in the rostral prosencephalon during development of the telencephalic and optic vesicles. *Neuroscience*. **108**:183–206.
85. Ohkubo, Y., Chiang, C., and Rubenstein, J.L. 2002. Coordinate regulation and synergistic actions of BMP4, SHH and FGF8 in the rostral prosencephalon regulate morphogenesis of the telencephalic and optic vesicles. *Neuroscience*. **111**:1–17.
86. Rallu, M., et al. 2002. Dorsoventral patterning is established in the telencephalon of mutants lacking both Gli3 and Hedgehog signaling. *Development*. **129**:4963–4974.
87. Willnow, T.E., et al. 1996. Defective forebrain development in mice lacking gp330/megalyn. *Proc. Natl. Acad. Sci. U. S. A.* **93**:8460–8464.
88. Spoelgen, R., et al. 2005. LRP2/megalyn is required for patterning of the ventral telencephalon. *Development*. **132**:405–414.
89. McCarthy, R.A., Barth, J.L., Chintalapudi, M.R., Knaak, C., and Argraves, W.S. 2002. Megalin functions as an endocytic sonic hedgehog receptor. *J. Biol. Chem.* **277**:25660–25667.
90. Morales, C.R., et al. 2006. Epithelial trafficking of Sonic hedgehog by megalin. *J. Histochem. Cytochem.* **54**:1115–1127.
91. Cole, F., and Krauss, R.S. 2003. Microform holoprosencephaly in mice that lack the Ig superfamily member Cdon. *Curr. Biol.* **13**:411–415.
92. Helms, J.A., Cordero, D., and Tapadia, M.D. 2005. New insights into craniofacial morphogenesis. *Development*. **132**:851–861.
93. Hu, D., and Helms, J.A. 1999. The role of sonic hedgehog in normal and abnormal craniofacial morphogenesis. *Development*. **126**:4873–4884.
94. Jeong, J., Mao, J., Tenzen, T., Kottmann, A.H., and McMahon, A.P. 2004. Hedgehog signaling in the neural crest cells regulates the patterning and growth of facial primordia. *Genes Dev.* **18**:937–951.
95. Seppala, M., et al. 2007. Gas1 is a modifier for holoprosencephaly and genetically interacts with sonic hedgehog. *J. Clin. Invest.* **117**:1575–1584.
96. Allen, B.L., Tenzen, T., and McMahon, A.P. 2007. The Hedgehog-binding proteins Gas1 and Cdo cooperate to positively regulate Shh signaling during mouse development. *Genes Dev.* **21**:1244–1257.
97. Park, H.L., et al. 2000. Mouse Gli1 mutants are viable but have defects in SHH signaling in combination with a Gli2 mutation. *Development*. **127**:1593–1605.
98. Hardcastle, Z., Mo, R., Hui, C.C., and Sharpe, P.T. 1998. The Shh signalling pathway in tooth development: defects in Gli2 and Gli3 mutants. *Development*. **125**:2803–2811.
99. Cheng, X., et al. 2006. Central roles of the roof plate in telencephalic development and holoprosencephaly. *J. Neurosci.* **26**:7640–7649.
100. Fernandes, M., Gutin, G., Alcorn, H., McConnell, S.K., and Hebert, J.M. 2007. Mutations in the BMP pathway in mice support the existence of two molecular classes of holoprosencephaly. *Development*. **134**:3789–3794.
101. Huang, X., Litingtung, Y., and Chiang, C. 2007. Ectopic sonic hedgehog signaling impairs telencephalic dorsal midline development: implication for human holoprosencephaly. *Hum. Mol. Genet.* **16**:1454–1468.
102. Chow, R.L., and Lang, R.A. 2001. Early eye development in vertebrates. *Annu. Rev. Cell Dev. Biol.* **17**:255–296.
103. Jeong, Y., El-Jaick, K., Roessler, E., Muenke, M., and Epstein, D.J. 2006. A functional screen for sonic hedgehog regulatory elements across a 1 Mb interval identifies long-range ventral forebrain enhancers. *Development*. **133**:761–772.
104. Storm, E.E., Rubenstein, J.L., and Martin, G.R. 2003. Dosage of Fgf8 determines whether cell survival is positively or negatively regulated in the developing forebrain. *Proc. Natl. Acad. Sci. U. S. A.* **100**:1757–1762.
105. Hayhurst, M., Gore, B.B., Tessier-Lavigne, M., and McConnell, S.K. 2008. Ongoing sonic hedgehog signaling is required for dorsal midline formation in the developing forebrain. *Dev. Neurobiol.* **68**:83–100.
106. Monuki, E.S. 2007. The morphogen signaling network in forebrain development and holoprosencephaly. *J. Neuropathol. Exp. Neurol.* **66**:566–575.
107. Marcucio, R.S., Cordero, D.R., Hu, D., and Helms, J.A. 2005. Molecular interactions coordinating the development of the forebrain and face. *Dev. Biol.* **284**:48–61.
108. Ming, J.E., and Muenke, M. 2002. Multiple hits during early embryonic development: digenic diseases and holoprosencephaly. *Am. J. Hum. Genet.* **71**:1017–1032.
109. Shen, J., and Walsh, C.A. 2005. Targeted disruption of Tgif, the mouse ortholog of a human holoprosencephaly gene, does not result in holoprosencephaly in mice. *Mol. Cell. Biol.* **25**:3639–3647.
110. Kuang, C., et al. 2006. Intragenic deletion of Tgif causes defects in brain development. *Hum. Mol. Genet.* **15**:3508–3519.
111. Brain Maps. http://www.brainmaps.org/ajax-viewer.php?datid=17&sname=epc20_hor
112. MedPix. http://rad.usuhs.mil/medpix/medpix_image.html?imageid=19795
113. Chen, L., et al. 2006. Cdc42 deficiency causes Sonic hedgehog-independent holoprosencephaly. *Proc. Natl. Acad. Sci. U. S. A.* **103**:16520–16525.